REBOUND ORIGINAL RESEARCH COMMUNICATION

Hydrogen Sulfide Mitigates Myocardial Infarction *via* Promotion of Mitochondrial Biogenesis-Dependent M2 Polarization of Macrophages

Lei Miao[1], Xiaoyan Shen[1], Matthew Whiteman[2], Hong Xin[1], Yaqi Shen[1], Xiaoming Xin[1], Philip K. Moore[3]andYi-Zhun Zhu[1,3]

[1]Department of Pharmacology, School of Pharmacy and Institutes of Biomedical Sciences, Fudan University, Shanghai, China, [2]University of Exeter Medical School, Exeter, UK, [3]Department of Pharmacology, Yoo Loo Lin School of Medicine, National University of Singapore, Singapore.

*Correspondence and requests for materials should be addressed to Y.Z.Z. (zhuyz@fudan.edu.cn), or X.Y.S. (shxiaoy@fudan.edu.cn)

Abstract

Aims: Macrophages are of key importance for tissue repair after myocardial infarction (MI). Hydrogen sulfide (H_2S) has been shown to exert cardioprotective effects in MI. However, the mechanisms by which H_2S modulates cardiac remodeling and repair post-MI remain to be clarified. ***Results:*** In our current study, we showed H_2S supplementation ameliorated pathological remodeling and dysfunction post-MI in WT and CSE-KO mice, resulting in decreased infarct size and mortality, accompanied by an increase in the number of M2-polarized macrophages at the early stage of MI. Strikingly, adoptive transfer of NaHS-treated bone marrow-derived macrophages (BMMs) into WT and CSE-KO mice with depleted macrophages also ameliorated MI-induced cardiac functional deterioration. Further mechanistic studies demonstrated that NaHS-induced M2 polarization was achieved by enhanced mitochondrial biogenesis and fatty acid oxidation (FAO). ***Innovation and Conclusion:*** Our study shows, for the first time, that H_2S may have the potential as a therapeutic agent for MI *via* promotion of M2 macrophage polarization. ***Rebound Track:*** This work was rejected during standard peer review and rescued by Rebound Peer Review (Antioxid Redox Signal 16:293–296, 2012) with the following serving as open re-viewers: Hideo Kimura, Chaoshu Tang, Xiaoli Tian and Kenneth Olson.

Keywords: Myocardial infarction; hydrogen sulfide; macrophage; polarization;

Innovation

We show here H_2S supplementation ameliorated pathological remodeling and dysfunction post-MI, accompanied by an increase in M2-polarized macrophages. And we present evidence for a novel mechanism by which macrophage polarization triggered by H_2S is due to the increase of mitochondrial biogenesis which enhanced lipolysis and fatty acid release, and provided the respiratory substrates for FAO. Our study shows for the first time that H_2S supplementation, such as H_2S donors or activators of H_2S biosynthesis could represent a promising novel therapeutic strategy for MI treatment via stimulation of M2 macrophage polarization.

Introduction

Myocardial infarction (MI) is one of the leading causes of morbidity and mortality globally (5,36). Accumulating evidence indicates that inflammatory reactions are essential events for the healing process and scar formation during post-infarction remodeling (21). Monocytes/macrophages are primary responders of inflammation and are of central importance for cardiac healing after MI at multiple levels (9). Macrophages, both in the steady-state and in disease, are derived mainly from monocytes and/or recruited from the bone marrow (27). During MI, macrophages infiltrate into the necrotic myocardium and this, as a part of a robust inflammatory response, is critical for the conversion of infarcted tissues into granulation tissues and for collagen scarring (40).

Macrophage activation (polarization) results in the generation of classically activated (M1) and alternatively activated (M2) subsets which exhibit distinct cell marker expression and diverse immunological functions (21). During the early inflammatory stage of MI, M1 macrophages rapidly infiltrate into the injury site and display a strong inflammatory phenotype by secreting large amounts of pro-inflammatory cytokines such as TNF-α, interleukin-1 (IL-1) and IL-6, which play key roles in the phagocytosis of cellular debris. However, if the pro-inflammatory response becomes excessive and goes uncontrolled, such beneficial behaviour becomes unwanted and leads to inhibition of the healing process in which a predominant transition from M1 toward M2 macrophage occurs (45). M2 macrophages are distinguished by the enriched expression of molecules such as IL-10, arginase 1 (Arg-1), and CD206 (35), leading to a dampened pro-inflammatory and enhanced anti-inflammatory phenotype to counteract excessive inflammation and initiate tissue regeneration (28,39). Thus, the prolonged dominance of M1 macrophages may be detrimental and impede the healing of the infarct after MI (37). In sharp contrast, M2-polarized macrophages have been suggested to mitigate cardiac functional deterioration and improve infarct repair during MI (27). Therefore, it has been proposed that clinical therapy of MI should include resolution of inflammation to balance the disposition of inflammatory and reparative macrophages (12,25).

Hydrogen sulfide (H_2S) has recently been proposed as a novel endogenous ‘gasomediator’ endogenously generated during cysteine metabolism, catalysed by cystathionine-β-synthase, cystathionine-γ-lyase (CSE) or 3-mercaptopyruvate sulfur transferase (33). CSE is thought to be the predominant source of H_2S in the cardiovascular system (24). Genetic or pharmacological inhibition of CSE exacerbates myocardial ischemia/reperfusion injury, highlighting the importance of endogenous H_2S in limiting cardiac injury (2,29). Conversely, H_2S supplementation has been shown to inhibit or reverse cardiac injury of various types, including MI, in which H_2S reduced infarct size and improved cardiac healing (6,15,19,20,31,42,44,47). Several mechanisms have been proposed to explain the cardioprotective function of H_2S, such as promotion of angiogenesis (19), protection against oxidative stress (44). However, the precise mechanisms for H_2S-modulated infarct repair and restoration of cardiac function post-MI are not completely understood. Given the critical role of macrophage polarization in MI, in the present study, we aimed to elucidate the impact of macrophage polarization on the cardioprotective effects of H_2S after MI and to investigate the mechanisms involved.

Rebound Track

This work was rejected during standard peer review and rescued by Rebound Peer Review (Antioxid Redox Signal 16:293–296, 2012) with the following serving as open re-viewers: Hideo Kimura, Chaoshu Tang, Xiaoli Tian and Kenneth Olson. The comments by these reviewers supporting the rescue are listed below:

Hideo Kimura (kimura@ncnp.go.jp): I am a qualified reviewer (per Antioxid Redox Signal. 16:293-6) and move to rescue this manuscript that was rejected during the regular peer review process after reviewing all versions of the manuscript and detailed reviewer comments. The authors studied the protective effect of H_2S on tissue repair after myocardial infarction focusing on the effect on macrophages. They found that H_2S decreased the infarct size and mortality by inducing macrophage polarization through enhanced mitochondrial biogenesis and fatty acid oxidation. Therefore, in the interest of science, I take full responsibility to rescue this work from rejection.

Chaoshu Tang (tangchaoshu@263.net.cn): I am a qualified reviewer (per Antioxid Redox Signal. 16:293-6) and move to rescue this manuscript that was rejected during the regular peer review process after reviewing all versions of the manuscript and detailed reviewer comments. The authors focus on M2 macrophage polarization induced by CSE/H_2S participation in protection of H_2S on post-MI. Author also observed that H_2S affected macrophage mitochondrial biogenesis and fatty acids oxidation. Thus, author make a conclusion that H_2S induced macrophage M2 polarization by mitochondrial biogenesis and fatty acids oxidation. It is an interesting work. However, there were some concerns which are now satisfactorily addressed by revision.

Xiaoli Tian (tianxiaoli@pku.edu.cn): I am a qualified reviewer (per Antioxid Redox Signal. 16:293-6) and move to rescue this manuscript that was rejected during the regular peer review process after reviewing all versions of the manuscript and detailed reviewer comments. It has been previously shown in various model organisms that H_2S has cardiac protective effects during myocardial infarction via an increased angiogenesis and anti-oxidative stress. Authors in this study presented that the cardioprotective effect was possibly achieved M2 polarization that is caused by NaSH-enhanced mitochondrial biogenesis and fatty acid oxidation. I think it is pretty interesting study that identified a novel mechanism underlying cardioprotective effect of H_2S. After revision in response to my concerns, I think the manuscript is overall solid.

Kenneth Olson (kolson@nd.edu): I am a qualified reviewer (per Antioxid Redox Signal. 16:293-6) and move to rescue this manuscript that was rejected during the regular peer review process after reviewing all versions of the manuscript and detailed reviewer comments. This is an extensive and relatively thorough study of the ability of hydrogen sulfide to selectively direct differentiation of M2 macrophages and thereby protect the heart from myocardial infarction. I had some reservations which have been satisfactorily addressed during revisions. I think this is a very good paper.

Results

NaHS mitigates cardiac functional deterioration following MI

The CSE null (KO) mice which lacking the H_2S-producing enzyme cystathionine γ-lyase were evaluated to detect the endogenous CSE level of the heart tissue. As shown by western blot result, the expression of CSE was depleted in KO mice compared to WT mice (Supplementary Fig. S1). In agreement with a recent report (43), H_2S levels in heart tissue from CSE KO mice were decreased (Fig. 1A). While, NaHS treatment could significantly increase the H_2S concentration in the heart tissue of both WT and CSE-KO mice (Supplementary Fig. S2). WT and CSE KO mice in different groups were subject to MI or sham surgery and survival over the following 8 days determined. In the WT-MI group, only 8 of 15 mice (53%) survived up to 8 days post-MI, while in the NaHS (2 mg/kg or 4 mg/kg) groups, 10 and 12 (67%, 80%) mice survived, respectively. In the CSE KO-MI group, 6 out of 15 mice (40%) survived up to 8 days post-MI. Thus, survival rate after MI was lower in CSE KO than in WT mice, thereby suggesting the importance of endogenous H_2S in protecting against MI (Fig. 1B and Supplementary Fig. S3A). Echocardiographic analysis revealed that CSE KO mice exhibited exacerbated pathological remodeling and functional deterioration after MI. Impressively, NaHS treatment in these animals significantly improved cardiac function in both WT and KO mice (Fig. 1C,D).

NaHS increases the percentage of anti-inflammatory M2 macrophages in the infarcted heart after MI

M1/M2 polarization during infiltration of macrophages is crucial for healing of the infarcted myocardium (7,11). To identify the effect of NaHS on polarization of infiltrating macrophages during cardiac remodeling, CD206, a M2-like macrophage marker (1), was first used to assess the phenotype of macrophages in heart tissues by immunohistochemical analysis. NaHS treatment significantly increased the density of CD206 staining 5 days after MI in both WT and CSE-KO mice (Fig. 2A). To confirm this, $CD11b^+$ cells separated from infarcted hearts were analyzed by flow cytometry. As shown in Fig. 2B, CSE KO decreased the percentage ($F4/80^+CD206^+$ cells) whilst, NaHS treatment increased the percentage of M2 but not M1 macrophages ($F4/80^+CD11c^+$ cells), in the infarcted hearts of WT and KO mice at day 3 with the effect peaking at day 5. The M2/M1 ratio revealed a similar trend (Fig. 2B). Furthermore, mRNA levels of the anti-inflammatory cytokine IL-10 and CD163 in macrophages extracted from infarcted LVs of KO mice were lower than those in WT mice and were elevated by NaHS treatment (Fig. 2C). In comparison with WT-MI mice, levels of the three M1 markers were increased in CSE KO animals and this effect was reduced by NaHS (Fig. 2D). Together, these data indicated that H_2S directs macrophages conversion towards the M2 phenotype in infarcted hearts shortly after MI.

NaHS induces M2 polarization of monocytes and macrophages

During the early stage of MI, circulating monocytes are recruited into infarcted tissue and

differentiate to macrophages (7). To track the effect of NaHS on monocytes, blood in the steady state and 5 days after MI (with/without NaHS treatment) in both WT and CSE KO mice was profiled and the subsets of monocyte population identified on the basis of the expression of Ly-6C and CX_3CR1 by FACS analysis (7). A slight increase of Ly-$6C^{low}CX_3CR1^{high}$ monocytes was detected in the MI group which was further increased by NaHS treatment at 5 days after MI (Supplementary Fig. S4).

To further confirm the effect of NaHS on M2 polarization, the phenotype of bone marrow-derived macrophages (BMMs) from WT and CSE KO mice with NaHS (2 mg/kg) treatment was analyzed. M2($F4/80^+CD206^+$) macrophage number was significantly increased by NaHS treatment for 12 h but declined at 24 h. Compared with WT, CSE KO mice displayed a decreased population of $F4/80^+CD206^+$BMMs, which maybe virtue of the decreased H_2S level (Supplementary Fig. S2B), but was rescued by NaHS treatment (Fig. 3A,B). Consistent with flow cytometry analysis, NaHS-treated-BMMs from both WT and KO mice showed a larger increase in M2 markers (Arg1, CD206, Ym1 and Fizz1) compared with NaHS-untreated BMMs (Fig. 3C). In contrast, although NaHS had no influence on the number of $F4/80^+Ly6C^+$ macrophages, as well as the mRNA level of M1 marker (CCR2, IL-12βand CCL3) (Supplementary Fig. S5A,B) this drug depressed IFN-γ-induced M1 polarization (Supplementary Fig. S5C,D). Collectively, these results suggest that H_2S triggers the polarization of macrophages to the anti-inflammatory M2 phenotype in BMMs isolated from both WT and KO mice, but not to the pro-inflammatory M1 macrophages.

NaHS-treated BMMs ameliorates cardiac functional deterioration following MI

To verify the cardioprotective role of M2-polarized macrophages *in vivo*, BMMs were treated with NaHS and then transplanted into WT and CSE KO mice in which endogenous macrophages have been depleted by treatment with clodronate liposome (13). We first verified the purity of BMMs using the macrophage surface marker F4/80, and found that 98.1% of the BMMs isolated from WT mice were F4/80 positive (Supplementary Fig. S6). Intravenous administration of clodronate liposome dramatically decreased CD68 staining confirming that endogenous macrophages had been effectively depleted (Fig. 4A). We next treated BMMs with NaHS *in vitro* for 12h, followed by *in vivo* adoptive transfusion to donor animals and MI. Remarkably, expression of CD206 was detected in the hearts of both WT and KO mice 3 days after MI (Fig. 4B). TTC staining was then performed to determinate myocardial infarct size. As shown in Fig. 4C,D, myocardial infarct size was reduced by NaHS-treated BMMs injection compared with untreated BMMs. Furthermore, echocardiography suggested a positive effect of NaHS-treated BMMs in hampering cardiac functional deterioration (Fig. 4E,F). Taken together, these results support the long-held assertion that macrophages play a key role in protecting myocardium against ischemia injury, and suggest that H_2S-induced M2-polarization of macrophages contributes to the cardioprotective effect of H_2S in MI.

NaHS accelerates fatty acid oxidation and lipolysis in M2 polarization of BMMs

Based on the observed cardioprotective effect of NaHS-induced M2 polarized BMMs in infarcted myocardium of both WT and CSE KO mice, we next focused our attention on the

mechanism of action of NaHS in macrophage polarization involved in myocardial preservation. Previous studies have suggested that M1-polarized macrophages get most of their energy by aerobic glycolysis while mitochondrial oxidative phosphorylation, fueled by fatty acid oxidation (FAO),is a key component of energy usage by M2-polarized macrophages (16). Therefore, we measured oxygen consumption in BMMs from WT and CSE KO exposed to NaHS for 12 h. Surprisingly, a significant increase in mitochondrial oxygen-consumption rate (OCR), spare respiratory capacity (SRC) and the ratio of oxidative phosphorylation to aerobic glycolysis (OCR/ECAR) was apparent in NaHS-treated WT BMMs. Moreover, reduced OCR and SRC occurred in BMMs from CSE KO mice c.f. WT BMMs and this deficiency was reversed by H_2S replacement with NaHS (Fig. 5A,B). In contrast, we found no change in BMM aerobic glycolysis, determined as the extracellular acidification rate (ECAR), following NaHS treatment (Supplementary Fig. S7), which is consistent with our earlier observation that NaHS does not affect M1 polarization (Supplementary Fig. S5A,B). Considering the close link between FAO and lipolysis of triacylglycerols stored in neutral lipids, we then measured the content of neutral lipids and found that this was also decreased by NaHS treatment (Fig. 5C,D). Moreover, the expression of Lipa, a lipase which is upregulated in M2 macrophages, was robustly increased in NaHS-treated BMMs (Fig. 5E), implying that the enhanced lipolysis and FAO may be responsible for NaHS-induced M2 polarization.

Fatty acid oxidation and lipolysis are essential for NaHS-induced M2 polarization

To validate the contribution of FAO and lipolysis to NaHS-induced M2 polarization, etomoxir, an inhibitor of mitochondrial oxygen consumption and tetrahydrolipistatin (orlistat), an inhibitor of lipolysis of triacylglycerols (16), were used. The NaHS-mediated rise in OCR, SRC and ratio of OCR to ECAR in treated BMMs were prevented by each inhibitor (Fig. 5F,G). Flow cytometry analyses also showed that both etomoxir and orlistat suppressed M2 polarization triggered by NaHS (Fig. 5H,I). Similarly, the up-regulation of M2 polarization-related genes (Arg1, CD206, Ym1 and Fizz1) was reduced by these inhibitors (Fig. 5J). Together, these data strongly suggest that mitochondrial FAO and lipolysis are essential for NaHS-induced M2 polarization.

Mitochondrial biogenesis is responsible for NaHS-induced M2 polarization

Mitochondrial biogenesis plays critical roles in energy homeostasis and metabolism (41). We next explored whether the enhanced FAO and lipolysis in NaHS-induced M2 polarization was due to mitochondrial biogenesis. Cellular mitochondrial mass was measured by staining BMMs with MitoFluor Green NaHS treatment for 12 h. Weak staining was observed in control BMMs not exposed to NaHS whilst NaHS markedly increased mitochondria staining both in WT and in CSE KO BMMs (Fig. 6A). This result was confirmed by flow cytometry (Fig. 6B,C). In addition, expression of genes involved in mitochondrial biogenesis (e.g. nuclear receptor PPARγ co-activator, PGC1β and PPARγ) were markedly upregulated by NaHS (Fig. 6D). Furthermore, translocation of PPARγ from cytoplasm to the nucleus was also observed in NaHS-treated BMMs (Fig. 6E) indicating activation of mitochondrial oxidative phosphorylation. In addition, the inhibitor of mitochondrial biogenesis, chloramphenicol (CAM), significantly

blocked NaHS-induced enhancement of fluorescence intensity (Fig. 6F). Importantly, pretreatment with CAM inhibited the surge of $F4/80^{+}CD206^{+}$ BMMs (Fig. 6G) and the up-regulation of M2 polarization-related genes induced by NaHS (Fig. 6H). Collectively, these data demonstrate that mitochondrial biogenesis fueling FAO is a key mediator in NaHS-induced M2 responsible.

Discussion

MI, one of the most lethal events globally, may result in heart failure if it does not end life immediately (27). Currently, there are no clinically applicable medications for myocardial ischemic injury (5). In the cardiovascular system, H_2S is formed via the cysteine enzymatic conversion by cystathionine-gamma-lyase (CSE). And, H_2S has been reported to play a role as a cardioprotectant in MI (4,33). In the current study, increased cardiac dysfunction and mortality post-MI was apparent in CSE-KO mice. In contrast, improved cardiac remodeling and function accompanied with decreased mortality was observed in both WT mice and CSE KO-MI mice treated with NaHS, suggesting that strategies to increase cardiac H_2S bioavailability may represent a novel and efficacious treatment for MI. Additionally, H_2S ameliorated myocardiac injury by promoting the transition of macrophages towards M2 phenotype, which is involved in the resolution of inflammation.

Inflammatory reactions triggered by myocardial necrosis post-MI clears the wound of dead cells and matrix debris and are believed to be critical for infarct healing, vascularization, and restoring cardiac function (21,27). Macrophages are the principle inflammatory cell type involved in the regulation of the healing process and modulate the inflammatory response to MI at multiple levels (18,21). Early in MI, Th1 cytokines, C-C chemokines promote classical activation of macrophages, exacerbating the inflammatory response and cardiac dysfunction (45). Subsequently, alternatively activated macrophages accumulate in the damaged tissue and initiate the repair process, since M2 macrophages antagonize pro-inflammatory responses and help to engulf cellular debris (26,38). In addition, considerable data demonstrates that switching between subsets of macrophages is important for cardiac healing after MI (3,46). In this study, we also show macrophages recruitment to the infarcted myocardium were driven by H_2S towards the M2 phenotype resulting in increased synthesis of anti-inflammatory cytokines and decreased generation of pro-inflammatory cytokines. These findings suggest a previously undiscovered mechanism underlying H_2S mediated cardioprotection.

It is well established that optimal healing of the myocardium involves the presence of inflammatory Ly-$6C^{high}$ monocytes/macrophages and later accumulation of reparative Ly-$6C^{low}$ monocytes/macrophages (14). Generally, monocytes originate from the bone marrow and then enter the blood and rapidly influx into tissue and differentiate to macrophages in injury (14,27). The blood profile data in our current study show that H_2S significantly increased the levels of anti-inflammatory Ly-$6C^{low}$ $CX3CR1^{high}$ monocytes in blood after MI, indicating that the cardiac protection of H_2S maybe contributed by the lowering of inflammatory monocytes and the upregulation of anti-inflammatory monocytes in the blood of MI mice. Consistent with these results, H_2S supplementation (e.g. using NaHS) polarized BMMs towards the anti-inflammatory M2 phenotype rather than pro-inflammatory M1 phenotype, confirming the

roles of H_2S in the differentiation of macrophages. By the *in vivo* macrophages depletion and adoptive transfer approach (32),we found NaHS-treated BMMs decreased the infarct size and ameliorated the cardiac functional deterioration after MI. These results further suggest that the cardioprotective effect of H_2S in MI were due to the induction of M2 polarization in macrophages.

It is now becoming clear that different macrophage phenotypes utilize cellular energy differently (16). M1 macrophages display a high energy state supported by up-regulation of aerobic glycolysis during the early stages of inflammation. The lipolysis of exogenous triacylglycerols stored in lipid droplets is required to generate fatty acids for FAO, which, in turn, is critical for IL-4-induced M2 polarization (16,30). The current study shows marked increase of FAO, as evaluated by OCR, OCR/ECAR and SRC, enhanced lipolysis in H_2S-induced M2 polarization. Inhibition of mitochondrial oxygen consumption or triacylglycerols lipolysis by etomoxir and orlistat suppressed H_2S-induced M2 polarization, indicating that FAO and lipolysis were essential for H_2S-induced M2 polarization. It has been reported that CSE, localized in the cytosol of vascular smooth-muscle cells on resting conditions, could transfer to mitochondria under some specific stress stimulations, and promote H_2S production inside to sustain mitochondrial ATP production. Inhibition of CSE activity leads to reduction of mitochondrial ATP production (10) and renders cells more prone to oxidative injury (8). Moreover, mitochondrial oxidative phosphorylation, as a primary source of ATP production, is indispensable for FAO and lipolysis (16). Therefore, these observations raise the possibility of a link between mitochondria and FAO during H_2S-induced M2 polarization.

Mitochondria, as the major site of oxidative energy production, are involved in numerous important intracellular events. Impaired mitochondrial function and biogenesis has been proposed to lead to and/or contribute to the development of numerous disorders (34). Mitochondrial mass is governed by a host of coordinate nucleus-encoded factors and coactivators during the process of cellular metabolism. For instance, PPARγ, a member of related nuclear receptors super-family, is involved in regulating mitochondrial metabolism and encoding peroxisomal FAO enzymes (23). PGC-1α, a member of PGC-1 family, was identified as a co-activator of PPARγ and plays a key role for mitochondrial biogenesis, including increasing mitochondrial mass and activating FAO-related genes (34).Moreover, as another member of PGC-1 family, PGC-1β has been reported to interact with and activate PGC-1α (22). Data from our current study in BMMs show a marked increase of mitochondrial mass following H_2S treated, concurring with the up-regulation of PPARγ and PGC-1β expression, indicating a new function of H_2S in mitochondrial biogenesis. Inhibition of mitochondrial biogenesis prevented the surge of M2-polarized macrophages, as well as the up-regulation of M2 polarization-related genes caused by NaHS. Thus, our present data could be concluded that mitochondrial biogenesis induced by NaHS promotes FAO and lipolysis, which further provides energy for M2 polarization in BMMs.

In conclusion, our study demonstrates for the first time that decreased endogenous H_2S as occurs in CSE KO mice impairs infarct healing and cardiac function post-MI and that therapeutic treatment of mice with H_2S ameliorated post-MI remodeling and dysfunction, resulting in decreased mortality. The favorable effects of H_2S on the infarcted myocardium can be attributed to promotion of macrophage M2 polarization. Furthermore, we present evidence for a novel mechanism by which macrophage polarization, triggered by H_2S, results from increased

mitochondrial biogenesis which promoted lipolysis and FAO, and provided the respiratory substrates needed for M2 polarization. Thus, activation of M2 macrophages by H_2S supplementation, such as H_2S donors or activators of H_2S biosynthesis could represent a promising novel therapeutic strategy for MI treatment.

Materials and Methods

Reagents and antibodies

H_2S was administered in the form of NaHS. NaHS, triphenyltetrazolium chloride (TTC) and pharmacological inhibitors (orlistat, etomoxir and chloramphenicol) were all obtained from Sigma-Aldrich. Cytoplasmic and nuclear protein Extraction Kit was purchased from Fermentas. M-CSF was obtained from Peprotech. MitoFluor Green and BODIPY from Molecular Probes (invitrogen), and DAPI from Beyotime. CD11b+ Microbeads (mouse) from Miltenyi Biotec. Following antibodies were used: anti-PPARγ, anti-Histone H3(Cell Signaling); anti-GAPDH (Bioworld); anti-CSE (Santa Cruz); anti-F4/80-PE, anti-CD206-APC, anti-CX3CR1-PE, anti-Ly6C-FITC (eBbioscience); anti-CD11c-FITC (Biolegend); anti-CD206 (Abcam).

Mice

Adult male C57BL/6 wild type (WT) mice and CSE null (KO) mice with the C57BL/6 background, were acquired from Shanghai Research Center for Model Organisms, were littermates obtained *via* heterozygous breeding during this study. Mice knockout of CSE were normal in growth rate and reproduction. All animal procedures were performed following the "Guide for the Care and Use of Laboratory Animals" published by the National Institutes of Health (NIH) and were approved by the ethics committee of Experimental Research, Shanghai Medical College, Fudan University.

Measurement of H_2S

The H_2S levels in the heart tissues and bone marrow-derived macrophages from WT mice and KO mice was measured as previously described with minor revision (17). In brief, 30 μL supernatant of heart tissues or BMMs were homogenized in ice- cold Tris-HCl (100 mmol/L, pH 8.5), and 70 μL monobromobimane reagent was added, vortexed away from light, and then added 10 μL 20% Formic acid, following by centrifugation at 12,000 g, 4°C for 20 min. The supernatant was used to detect H_2S concentration by reverse-phase(RP)-HPLC analysis. Meanwhile, the protein in the supernatant of each group was quantified by BCA reagent. The H_2S concentrations determined using a curve created with sodium sulfide (0-40 μmol/L) standards were expressed as μmol/L. And the H_2S concentrations in heart tissues were expressed as μmol/g protein.

MI surgery

The left coronary artery was ligated permanently to induce myocardial ischemia as

previously described (6). Briefly, mice were anesthetized with isoflurane, intubated using a 20-gauge intravenous catheter with a blunt end, and ventilated with a standard rodent ventilator. The animal was turned onto its right side, and the chest hair was removed using hair removal cream. The thoracic cavity was opened in the third intercostal space and a 7-0 prolene suture placed at 1-2 mm distal to left atrium was used for permanent ligation. The chest was closed in layers, and the skin was sterilized with povidone iodine. Infarction was confirmed by observing LV blanching on the electrocardiogram. Thoracotomy was performed on sham-operated animals, and the pericardium only was opened, with no ligation around the left anterior descending artery.

Treatment protocols

The WT and CSE KO mice were randomly assigned into four treatment groups respectively: sham vehicle (saline) (n = 15), MI treated with vehicle (n = 15), MI treated with NaHS (2 mg/kg/day) diluted in saline (n = 15), and MI treated with NaHS (4 mg/kg/day) (n = 15). NaHS (2 mg/kg, 4 mg/kg) were administered intraperitoneally for 7 days before and for 3, 5, 8 days after MI. During the treatment period, the dosage of NaHS was adjusted according to the body weight. The death of animals was recorded every day.

For the transplantation of BMM-derived macrophages, WT and CSE KO mice were firstly depleted macrophages by administration of clodronate (CL_2MDP) liposomes, both groups were then randomly assigned into two treatment groups, injected intravenously with non-treated BMMs (n = 12) or NaHS-treated BMMs (n = 12), respectively. In addition, PBS liposomes were also administrated for both groups as a negative control. Infarct size and echocardiography were measured at day3 and day 5 respectively as described below.

Echocardiography

Mice in each group were anesthetized with 1-2% isoflurane in a 100% oxygen mix and placed on a heating pad. Transthoracic echocardiography was dynamically evaluated using Vevo770 (Visual Sonics Inc., Toronto, Canada) with a 716 probe. All images were acquired at heart rates > 400 bpm to achieve physiologically relevant measurements. The transducers with frequency of 10-MHz for ventricular structure provided spatial resolutions. Left ventricular internal dimension in systole (LVIDs) was obtained from the M-mode tracings, while other parameters such as left ventricular volume in systole (LVs), ejection fraction (EF) and fractional shortening (FS) were derived automatically by the High-Resolution Electrocardiograph system.

Infarct size measurement

Myocardial infarct size was determined by staining with 1% Triphenyltetrazolium chloride (TTC). In short, murine hearts in each group were rapidly excised three days after the MI surgery, and serially sliced into five equally thick sections, these sections were subsequently incubated in PBS containing TTC for 15 min at 37°C, and then digitally photographed. Infarction size was calculated as a ratio of the infarct area and the left ventricle, and images

assessed by Image J software (NIH, Boston, USA).

Immunohistochemistry

The hearts from sacrificed animals were excised immediately, and then fixed in 4% paraformaldehyde. Each heart was embedded in paraffin, sectioned at 5 μm. Immunohistochemical staining was performed with an EnVision Kit (Dako, Carpinteria, CA, USA). Specific antibodies were used to selectively detect different subsets of macrophages. No primary and IgG-matched isotype antibodies were used as negative controls.

Macrophage isolation from heart tissues

Macrophages in LV infarct area were isolated as previously described (45). Briefly, LV tissue from WT (n = 8) and KO (n = 8) was minced and dissociated into single cell suspension using collagen IV. Cells were washed and re-suspended, and then adjusted to a proper concentration for incubating with $CD11b^+$ microbeads. The positive cells were isolated for Real-time PCR using magnetic MS columns according to the manufacturer's specifications. For flow cytometry analysis, the isolated macrophages were further incubated indicated antibodies at 4 °C for 45 min.

Preparation of macrophages from bone marrow

Bone marrow-derived macrophages (BMMs) was isolated from femurs and tibias of 10-to12-week-old WT and CSE KO mice, and then cultured in RPMI 1640 medium supplemented with 10% FBS, 1% penicillin/streptomycin for overnight. Non-adherent cells were collected and plated in the medium containing 10 ng/ml recombinant murine M-CSF. After differentiation for 7 days, cells were either untreated or incubated with NaHS for different time points and pharmacological inhibitors were also applied to the BMMs.

Real-time PCR

Total RNA was extracted from the isolated LV infarct macrophages or BMMs of each group using TRIzol (Takara, Dalian, China), and cDNA was synthesized using the RevertAid^{TM} First Strand cDNA Synthesis Kit #1622 (Fermentas, Vilnius, Lithuania). To further determine the LV macrophage phenotype, M1 markers (IL-1β, TNF-α, IL-6,CCR2, IL12β, CCL3) and M2 markers (IL-10, CD163, Arg1, CD206, Ym1, Fizz1), as well as genes involved energy metabolism(PGC1β, PPARγ and Lipa), were evaluated by quantitative real-time PCR using SYBR Green I (Takara). The primer sequences of the genes were listed in Table 1 or described previously (45).

Flow cytometry

To assess macrophage subsets and the effects of NaHS on macrophage polarization, $CD11b^+$ macrophages from infarct LV were isolated respectively as previously described (22).

Flow cytometric identification was executed using combinations of the following mAbs: F4/80-PE, CD206-APC and CD11c-FITC; F4/80-PE, CD206-APC and Ly6C-FITC, The subsets of monocytes in blood were identified by labeling with Ly6C-FITC and CX3CR1-PE. In addition, the quantity of neutral lipids and mitochondrial biogenesis were also detected by staining with BODIPY and MitoFluor Green, respectively. Flow cytometry analysis was performed on a FACSCalibur instrument (BD Biosciences) equipped with Cell Quest software.

Immunofluorescence and confocal microscopy

BMMs from WT or KO mice plated onto glass covers lips were treated with NaHS for 12 h. The cells were incubated with MitoFluor Green for mitochondrial staining and DAPI (blue) for nucleus staining. Confocal laser scanning was carried out by Zeiss710 confocal imaging system, and five different areas of each section were observed.

Cytoplasmic and Nuclear protein isolation

Cytoplasmic and nuclear proteins were extracted using a ProteoJET cytoplasmic and nuclear protein Extraction Kit (Fermentas) following the manufacturer's instructions. Protein concentration was quantified using a BCA protein assay kit (Beyotime).

Western blot

Equal amounts of proteins were separated on SDS-PAGE and transferred to nitrocellulose membranes, followed by incubation with appropriate primary and secondary antibodies. Blots were developed by Immobilon^{TM} western Chemiluminescent HRP Substrate (Millipore).

Cellular bioenergetics assays

The metabolism assays were conducted as previously described with modifications (45). BMMs form WT and CSE KO mice were treated with NaHS (50 μM) with or without orlistat for 12h. After that time, etomoxir was added into the NaHS-treated group 15 minutes prior to analysis. Oligomycin (2 μg/ml) and FCCP (50 nM) were then applied to each group sequentially according the time point during the assay. The mitochondrial oxygen-consumption rate (OCR), spare respiratory capacity (SRC) and extracellular acidification rate (ECAR) were analyzed in real time using an XF-96 Extracellular Flux Analyzer (Seahorse Bioscience). OCR and ECAR rates were normalized to cellular protein content.

Statistical analyses

All data are expressed as mean ± SEM. All calculations were performed with the GraphPad Prism version 5.0. Differences between groups were analyzed using Student's t-test when only two groups were compared, or assessed by one-way analysis of variance with Tukey's post-hoc test when more than two groups were compared. Kaplan-Meier survival curves were compared by use of a log-rank test. A value of $P < 0.05$ was considered statistically significant.

Acknowledgments

This work was funded by the Key Program of National Nature Science Foundation of China (No.81330080) and the Key Program of Shanghai Committee of Science and Technology in China (No. 14JC1401100).

Author contributions

L.M., X.-Y.S. and Y.Z.Z. designed the research; L.M. performed most of the experiments and wrote the manuscript. H.X., Y.-Q.S., performed experiments and analyzed the data. X.-M.X. performed array analysis. X.-Y.S. and Y.Z.Z. supervised the work and helped write the manuscript. MW and PKM contributed to manuscript preparation and data analysis.

Author Disclosure Statement

The authors declare that they have no conflict of interest.

References

1. Ben-Mordechai T, Holbova R, Landa-Rouben N, Harel-Adar T, Feinberg MS, Abd Elrahman I, Blum G, Epstein FH, Silman Z, Cohen S, Leor J. Macrophage subpopulations are essential for infarct repair with and without stem cell therapy. *J Am Coll Cardiol* 62: 1890-901, 2013.
2. Calvert JW, Coetzee WA, Lefer DJ. Novel insights into hydrogen sulfide--mediated cytoprotection. *Antioxid Redox Signal* 12: 1203-17, 2010.
3. Cho DI, Kim MR, Jeong HY, Jeong HC, Jeong MH, Yoon SH, Kim YS, Ahn Y. Mesenchymal stem cells reciprocally regulate the M1/M2 balance in mouse bone marrow-derived macrophages. *Exp Mol Med* 46: e70, 2014.
4. Chuah SC, Moore PK, Zhu YZ. S-allylcysteine mediates cardioprotection in an acute myocardial infarction rat model via a hydrogen sulfide-mediated pathway. *Am J Physiol Heart Circ Physiol* 293: H2693-701, 2007.
5. Downey JM, Cohen MV. Why do we still not have cardioprotective drugs? *Circ J* 73: 1171-7, 2009.
6. Elrod JW, Calvert JW, Morrison J, Doeller JE, Kraus DW, Tao L, Jiao X, Scalia R, Kiss L, Szabo C, Kimura H, Chow CW, Lefer DJ. Hydrogen sulfide attenuates myocardial ischemia-reperfusion injury by preservation of mitochondrial function. *Proc Natl Acad Sci U S A* 104: 15560-5, 2007.
7. Fernandez-Velasco M, Gonzalez-Ramos S, Bosca L. Involvement of monocytes/macrophages as key factors in the development and progression of cardiovascular diseases. *Biochem J* 458: 187-93, 2014.
8. Fox B, Schantz JT, Haigh R, Wood ME, Moore PK, Viner N, Spencer JP, Winyard PG, Whiteman M. Inducible hydrogen sulfide synthesis in chondrocytes and mesenchymal progenitor cells: is H2S a novel cytoprotective mediator in the inflamed joint? *J Cell Mol Med* 16: 896-910, 2012.
9. Frantz S, Hofmann U, Fraccarollo D, Schafer A, Kranepuhl S, Hagedorn I, Nieswandt B, Nahrendorf M, Wagner H, Bayer B, Pachel C, Schon MP, Kneitz S, Bobinger T, Weidemann F,

Ertl G, Bauersachs J. Monocytes/macrophages prevent healing defects and left ventricular thrombus formation after myocardial infarction. *FASEB J* 27: 871-81, 2013.

10. Fu M, Zhang W, Wu L, Yang G, Li H, Wang R. Hydrogen sulfide (H2S) metabolism in mitochondria and its regulatory role in energy production. *Proc Natl Acad Sci U S A* 109: 2943-8, 2012.
11. Gordon S, Martinez FO. Alternative activation of macrophages: mechanism and functions. *Immunity* 32: 593-604, 2010.
12. Gordon S, Taylor PR. Monocyte and macrophage heterogeneity. *Nat Rev Immunol* 5: 953-64, 2005.
13. Harel-Adar T, Ben Mordechai T, Amsalem Y, Feinberg MS, Leor J, Cohen S. Modulation of cardiac macrophages by phosphatidylserine-presenting liposomes improves infarct repair. *Proc Natl Acad Sci U S A* 108: 1827-32, 2011.
14. Hilgendorf I, Gerhardt LM, Tan TC, Winter C, Holderried TA, Chousterman BG, Iwamoto Y, Liao R, Zirlik A, Scherer-Crosbie M, Hedrick CC, Libby P, Nahrendorf M, Weissleder R, Swirski FK. Ly-6Chigh monocytes depend on Nr4a1 to balance both inflammatory and reparative phases in the infarcted myocardium. *Circ Res* 114: 1611-22, 2014.
15. Huang C, Kan J, Liu X, Ma F, Tran BH, Zou Y, Wang S, Zhu YZ. Cardioprotective effects of a novel hydrogen sulfide agent-controlled release formulation of S-propargyl-cysteine on heart failure rats and molecular mechanisms. *PLoS One* 8: e69205, 2013.
16. Huang SC, Everts B, Ivanova Y, O'Sullivan D, Nascimento M, Smith AM, Beatty W, Love-Gregory L, Lam WY, O'Neill CM, Yan C, Du H, Abumrad NA, Urban JF, Jr., Artyomov MN, Pearce EL, Pearce EJ. Cell-intrinsic lysosomal lipolysis is essential for alternative activation of macrophages. *Nat Immunol* 15: 846-55, 2014.
17. Jin S, Pu SX, Hou CL, Ma FF, Li N, Li XH, Tan B, Tao BB, Wang MJ, Zhu YC. Cardiac H2S Generation Is Reduced in Ageing Diabetic Mice. *Oxid Med Cell Longev* 2015: 758358, 2015.
18. Kakio T, Matsumori A, Ono K, Ito H, Matsushima K, Sasayama S. Roles and relationship of macrophages and monocyte chemotactic and activating factor/monocyte chemoattractant protein-1 in the ischemic and reperfused rat heart. *Lab Invest* 80: 1127-36, 2000.
19. Kan J, Guo W, Huang C, Bao G, Zhu Y, Zhu YZ. S-propargyl-cysteine, a novel water-soluble modulator of endogenous hydrogen sulfide, promotes angiogenesis through activation of signal transducer and activator of transcription 3. *Antioxid Redox Signal* 20: 2303-16, 2014.
20. Kondo K, Bhushan S, King AL, Prabhu SD, Hamid T, Koenig S, Murohara T, Predmore BL, Gojon G, Sr., Gojon G, Jr., Wang R, Karusula N, Nicholson CK, Calvert JW, Lefer DJ. H(2)S protects against pressure overload-induced heart failure via upregulation of endothelial nitric oxide synthase. *Circulation* 127: 1116-27, 2013.
21. Lambert JM, Lopez EF, Lindsey ML. Macrophage roles following myocardial infarction. *Int J Cardiol* 130: 147-58, 2008.
22. Lin J, Puigserver P, Donovan J, Tarr P, Spiegelman BM. Peroxisome proliferator-activated receptor gamma coactivator 1beta (PGC-1beta), a novel PGC-1-related transcription coactivator associated with host cell factor. *J Biol Chem* 277: 1645-8, 2002.
23. Madrazo JA, Kelly DP. The PPAR trio: regulators of myocardial energy metabolism in health and disease. *J Mol Cell Cardiol* 44: 968-75, 2008.
24. Mani S, Li H, Untereiner A, Wu L, Yang G, Austin RC, Dickhout JG, Lhotak S, Meng QH, Wang R. Decreased endogenous production of hydrogen sulfide accelerates atherosclerosis.

Circulation 127: 2523-34, 2013.

25. Mantovani A, Biswas SK, Galdiero MR, Sica A, Locati M. Macrophage plasticity and polarization in tissue repair and remodelling. *J Pathol* 229: 176-85, 2013.
26. Martinez FO, Helming L, Gordon S. Alternative activation of macrophages: an immunologic functional perspective. *Annu Rev Immunol* 27: 451-83, 2009.
27. Nahrendorf M, Swirski FK. Monocyte and macrophage heterogeneity in the heart. *Circ Res* 112: 1624-33, 2013.
28. Nahrendorf M, Swirski FK, Aikawa E, Stangenberg L, Wurdinger T, Figueiredo JL, Libby P, Weissleder R, Pittet MJ. The healing myocardium sequentially mobilizes two monocyte subsets with divergent and complementary functions. *J Exp Med* 204: 3037-47, 2007.
29. Pan LL, Liu XH, Gong QH, Yang HB, Zhu YZ. Role of cystathionine gamma-lyase/hydrogen sulfide pathway in cardiovascular disease: a novel therapeutic strategy? *Antioxid Redox Signal* 17: 106-18, 2012.
30. Prieur X, Mok CY, Velagapudi VR, Nunez V, Fuentes L, Montaner D, Ishikawa K, Camacho A, Barbarroja N, O'Rahilly S, Sethi JK, Dopazo J, Oresic M, Ricote M, Vidal-Puig A. Differential lipid partitioning between adipocytes and tissue macrophages modulates macrophage lipotoxicity and M2/M1 polarization in obese mice. *Diabetes* 60: 797-809, 2011.
31. Qipshidze N, Metreveli N, Mishra PK, Lominadze D, Tyagi SC. Hydrogen sulfide mitigates cardiac remodeling during myocardial infarction via improvement of angiogenesis. *Int J Biol Sci* 8: 430-41, 2012.
32. Ranganathan PV, Jayakumar C, Ramesh G. Netrin-1-treated macrophages protect the kidney against ischemia-reperfusion injury and suppress inflammation by inducing M2 polarization. *Am J Physiol Renal Physiol* 304: F948-57, 2013.
33. Renga B. Hydrogen sulfide generation in mammals: the molecular biology of cystathionine-beta- synthase (CBS) and cystathionine-gamma-lyase (CSE). *Inflamm Allergy Drug Targets* 10: 85-91, 2011.
34. Scarpulla RC, Vega RB, Kelly DP. Transcriptional integration of mitochondrial biogenesis. *Trends Endocrinol Metab* 23: 459-66, 2012.
35. Schmidt T, Carmeliet P. Blood-vessel formation: Bridges that guide and unite. *Nature* 465: 697-9, 2010.
36. Sutton MG, Sharpe N. Left ventricular remodeling after myocardial infarction: pathophysiology and therapy. *Circulation* 101: 2981-8, 2000.
37. Swirski FK, Nahrendorf M. Leukocyte behavior in atherosclerosis, myocardial infarction, and heart failure. *Science* 339: 161-6, 2013.
38. Tabas I. Macrophage death and defective inflammation resolution in atherosclerosis. *Nat Rev Immunol* 10: 36-46, 2010.
39. Troidl C, Mollmann H, Nef H, Masseli F, Voss S, Szardien S, Willmer M, Rolf A, Rixe J, Troidl K, Kostin S, Hamm C, Elsasser A. Classically and alternatively activated macrophages contribute to tissue remodelling after myocardial infarction. *J Cell Mol Med* 13: 3485-96, 2009.
40. van Amerongen MJ, Harmsen MC, van Rooijen N, Petersen AH, van Luyn MJ. Macrophage depletion impairs wound healing and increases left ventricular remodeling after myocardial injury in mice. *Am J Pathol* 170: 818-29, 2007.
41. Vega RB, Horton JL, Kelly DP. Maintaining ancient organelles: mitochondrial biogenesis and maturation. *Circ Res* 116: 1820-34, 2015.

42. Wang Y, Zhao X, Jin H, Wei H, Li W, Bu D, Tang X, Ren Y, Tang C, Du J. Role of hydrogen sulfide in the development of atherosclerotic lesions in apolipoprotein E knockout mice. *Arterioscler Thromb Vasc Biol* 29: 173-9, 2009.

43. Yang G, Wu L, Jiang B, Yang W, Qi J, Cao K, Meng Q, Mustafa AK, Mu W, Zhang S, Snyder SH, Wang R. H2S as a physiologic vasorelaxant: hypertension in mice with deletion of cystathionine gamma-lyase. *Science* 322: 587-90, 2008.

44. Yang G, Zhao K, Ju Y, Mani S, Cao Q, Puukila S, Khaper N, Wu L, Wang R. Hydrogen sulfide protects against cellular senescence via S-sulfhydration of Keap1 and activation of Nrf2. *Antioxid Redox Signal* 18: 1906-19, 2013.

45. Zamilpa R, Kanakia R, Cigarroa Jt, Dai Q, Escobar GP, Martinez H, Jimenez F, Ahuja SS, Lindsey ML. CC chemokine receptor 5 deletion impairs macrophage activation and induces adverse remodeling following myocardial infarction. *Am J Physiol Heart Circ Physiol* 300: H1418-26, 2011.

46. Zhou LS, Zhao GL, Liu Q, Jiang SC, Wang Y, Zhang DM. Silencing collapsin response mediator protein-2 reprograms macrophage phenotype and improves infarct healing in experimental myocardial infarction model. *J Inflamm (Lond)* 12: 11, 2015.

47. Zhu YZ, Wang ZJ, Ho P, Loke YY, Zhu YC, Huang SH, Tan CS, Whiteman M, Lu J, Moore PK. Hydrogen sulfide and its possible roles in myocardial ischemia in experimental rats. *J Appl Physiol (1985)* 102: 261-8, 2007.

Abbreviations Used

Arg1 = arginase 1
BCA = bicinchoninic acid
BMMs = bone marrow-derived macrophages
CAM = chloramphenicol
CCL3 = chemokine (C-C motif) ligand 3
CCR2 = chemokine (C-C motif) receptor 2
CSE = cystathionine-γ-lyase
DAPI = 4,6'-diamidino-2'-phenylindole
ECAR = extracellular acidification rate
EF = ejection fraction
FS = fractional shortening
LVID, d = left ventricular internal dimension diastole
LVID, s = left ventricular internal dimension systole
SPRC = S-propargyl-cysteine
FAO = fatty acid oxidation
H_2S = hydrogen sulfide
IL-1 = interleukin-1
KO = knockout
Lipa = lysosomal acid lipase A
MI = myocardial infarction
OCR = oxygen-consumption rate
PPAR = peroxisome proliferator-activated receptor
PGC-1β = PPARγ-coactivator-1β

SRC = spare respiratory capacity
TNF = tumor necrosis factor
TTC = triphenyltetrazolium chloride
WT = wild type

Figure legends

FIG. 1.NaHS preserved cardiac function following MI. (**A**) Endogenous H_2S concentration in the heart tissue of WT mice and CSE-KO mice (n = 6). Data are expressed as mean ± SEM. (**B**) Kaplan-Meier survival curve of the indicated groups (n = 15). (**C**) Representative echocardiographic records obtained from mid-ventricular short-axis views of murine hearts (n = 12). (**D**) Statistical analysis of the data obtained or derived from original echocardiographic records. *P < 0.05, **P < 0.01 versus WT-MI group; $^{\#}$P < 0.05, $^{\#\#}$P < 0.01, $^{\#\#\#}$P < 0.01 versus KO-MI group (EF, represents: ejection fraction; FS represents: fractional shortening; LVID, d, represents: left ventricular internal dimension diastole; LVID, s represents: left ventricular internal dimension systole).

FIG.2.NaHS increased the number of anti-inflammatory M2 macrophages in LV after MI. (**A**) Representative images of CD206 staining after 5 days of post-MI treatment with NaHS in both WT and CSE-KO mice. Scale bars, 50 μm. (**B**)Flow cytometry analysis of macrophage polarization after treatment of NaHS (50 μM) for the indicated time post-MI. Top: the percentage of M1 macrophages not altered by NaHS. Middle: NaHS increased the percentage of M2 macrophages. Bottom: NaHS increased the ratio of M2/M1. (**C-D**) The mRNA levels of M2 macrophage markers (IL-10, CD163) (C) and M1 macrophage markers (IL-1β, IL-6, TNF-α) (D) in LV of WT and KO mice without or with NaHS (50 μM) treatment post-MI measured by real-time PCR.*P < 0.05, **P < 0.01 versus WT-MI group. $^{\#}$P < 0.05, $^{\#\#}$P < 0.01 versus KO-MI group.

FIG.3.NaHS induced M2 polarization of BMMs, isolated from WT and CSE-KO mice.(**A**) Expression of F4/80 and CD206 in BMMs treated with NaHS (2 mg/kg) for different time points, was assessed by flow cytometry. (**B**) Statistical analysis of the percentage of $F4/80^{+}CD206^{+}$ BMMs. (**C**) The mRNA levels of M2-related cytokines (Arg-1, CD206, Ym1 and Fizz1) in BMMs measured using RT real-time PCR. *P < 0.05, **P < 0.01 versus WT-BMMs group;$^{\#}$P < 0.05, $^{\#\#}$P < 0.01 versus KO-BMMs group.

FIG.4.Adoptive transfer of NaHS-treated BMMs ameliorated cardiac functional deterioration following MI. (**A**) Immunohistochemistry showed that the expression of macrophage marker CD68 was depleted in the heart of mice injected with clodronate liposome after MI. (**B**) After macrophage depletion with clodronate liposome, WT and CSE-KO mice were injected with NaHS-treated (50 μM) BMMs followed by MI. After 3 days, the expression of CD206 in the heart of indicated groups was detected by immunohistochemistry. (**C**) Representative heart images of TTC staining from indicated groups. (**D**) The infarct size is calculated by the ratio of the infarct area and left ventricle (n=10). (**E**) Representative echocardiographic records revealed that adoptive transfer of NaHS-treated BMMs ameliorated cardiac functional deterioration following MI. (**F**) Statistical analysis of the data obtained or derived from original echocardiographic records as shown in E. *P < 0.05, **P < 0.01 versus WT-MI group; $^{\#}$P < 0.05, $^{\#\#}$P < 0.01 versus KO-MI group.

FIG.5.Fatty acid oxidation and lipolysis were essential for NaHS-induced M2 polarization.

(**A**) Basal OCR of BMMs cultured without or with NaHS (50 μM) for 12 h, followed by sequential treatment with oligomycin (Oligo), FCCP, or rotenone plus antimycin (Rot + ant). (**B**) Graphic analysis of OCR, SRC, and the ratio of OCR to ECAR. (**C-D**) Neutral lipids of each group were measured by incubating with the fluorescent dye BODIPY, followed by flow cytometry analysis. The quantification of fluorescence intensity is shown. (**E**) The mRNA level of Lipa (lipolysis-related gene) in each group was measured by RT real-time PCR. *P < 0.05, **P < 0.01 versus WT-BMMs group; $^{\#}$P < 0.05, $^{\#\#}$P < 0.01 versus KO-BMMs group. (**F**) Basal OCR of WT-BMMs with the treatment of NaHSor NaHS plus the etomoxir (theinhibitor of FAO) or orlistat (the inhibitor of lipase). (**G**) Graphic analysis of the original records. The increased OCR, SRC and ratio of OCR to ECAR of BMMs were inhibited by etomoxir or orlistat. (**H**)Flow cytometry analysis showed the population of F4/80^{+}CD206^{+} WT-BMMs with the indicated treatment. (**I**) Statistical analysis revealed that the increased F4/80^{+}CD206^{+} macrophages caused by NaHS treatment was decreased by etomoxir or orlistat. (**J**) The mRNA levels of Arg1, CD206, Ym1 and Fizz1 in the indicated groups were measured by RT real-time PCR.*P < 0.05, **P < 0.01 versus Con group; $^{\#}$P < 0.05,$^{\#\#}$P <0.01 versus NaHS group.

FIG.6.Mitochondrial biogenesis is crucial for NaHS-induced M2 polarization. (**A**) WT or KO BMMs were treated with NaHS (50 μM) for 12 h, and then subjected to immunofluorescence analysis after MitoFluor Green labeling. Scale bar, 50 μm. (**B-C**) The fluorescence intensity of each group was evaluated by flow cytometry. (**D**) The mRNA levels of mitochondrial biogenesis-related genes (PGC1β and PPARγ) in the indicated group were measured by RT-real-time PCR. (E) The expressions of PPARγ in the nucleus and cytoplasm were analyzed by western blot. *P < 0.05, **P < 0.01 versus WT-BMMs group; $^{\#}$P < 0.05, $^{\#\#}$P < 0.01 versus KO-BMMs group. (**F**) The increased fluorescence intensity of BMMs treated by NaHS was blocked by mitochondrial biogenesis inhibitor chloramphenicol (CAM, 100 μM). (**G**) Flow cytometry analysis showed the increased F4/80^{+}CD206^{+} macrophages caused by NaHS treatment was decreased by CAM. (**J**) The mRNA levels of Arg1, CD206, Ym1 and Fizz1 in the indicated groups were evaluated by RT real-time PCR.*P < 0.05, **P < 0.01 versus Con group; $^{\#}$P < 0.05, $^{\#\#}$P <0.01 versus NaHS group.

Table 1. Real-time PCR primer sequences.

Gene	Forward (5'-3')	Reverse (5'-3')
IL-1β	CTCGTGCTGTCGGACCCAT	CAGGCTTGTGCTCTGCTTGTGA
IL-6	GACAAAGCCAGAGTCCTTCAGAGAG	CTAGGTTTGCCGAGTAGATCTC
IL-10	CAGTGGAGCAGGTGAAGAGTGA	CCTGGAGTCCAGCAGACTCAAT
TNF-α	ATGAGCACAGAAAGCATGATC	TACAGGCTTGTCACTCGAATT
CD163	CCAAGCTGTGAAGGCACTAAA	ACGGTTTGGCAGGACAATC
Lipa	GGAAACAGCAGAGGAAACACCT	CACGGGAGCCAAGACTAAAAC
CD206	GGATTGTGGAGCAGATGGAAG	CTTGAATGGAAATGCACAGA
Arg-1	CTCCAAGCCAAAGTCCTTAGAG	AGGAGCTGTCATTAGGGACATC
β-actin	AAGGCCAACCGTGAAAAGAT	GTGGTACGACCAGAGGCATAC

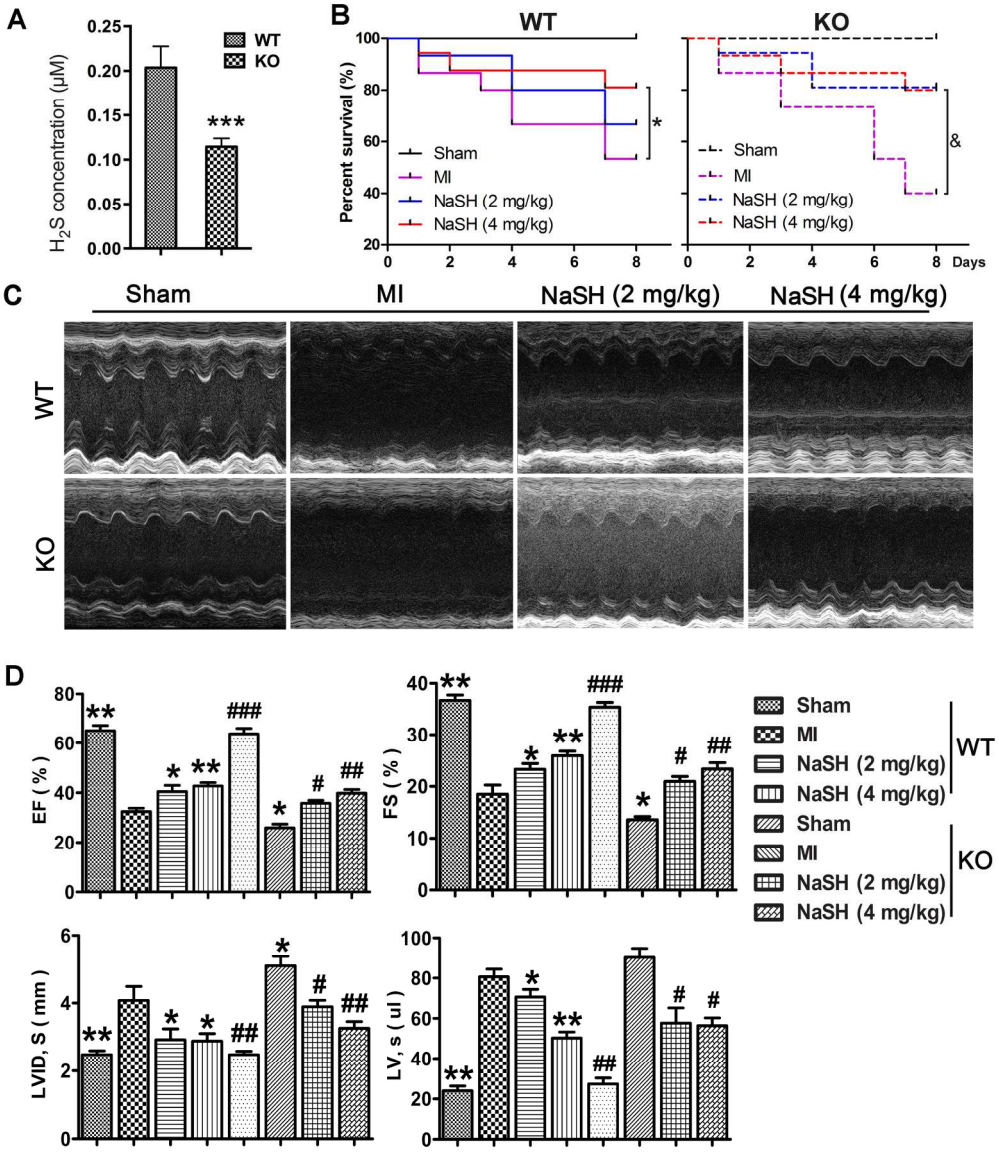

205x241mm (300 x 300 DPI)

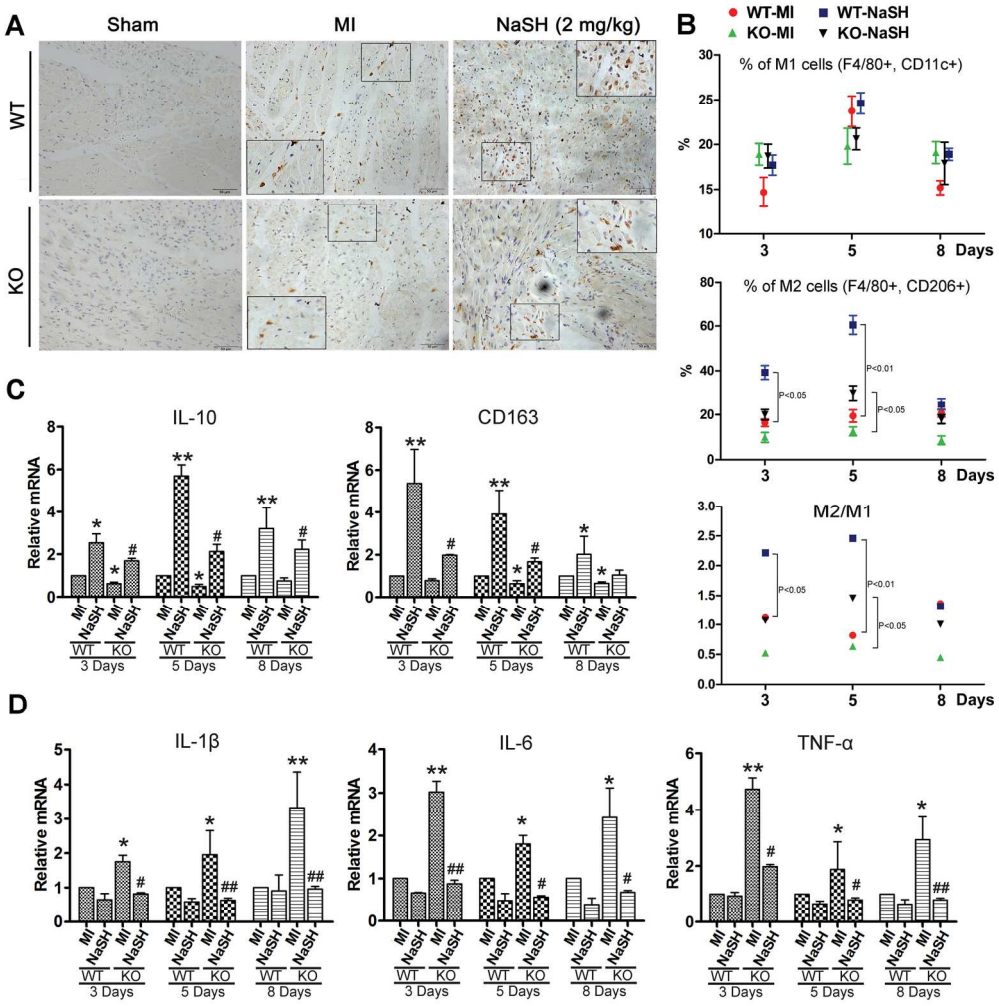

175x176mm (300 x 300 DPI)

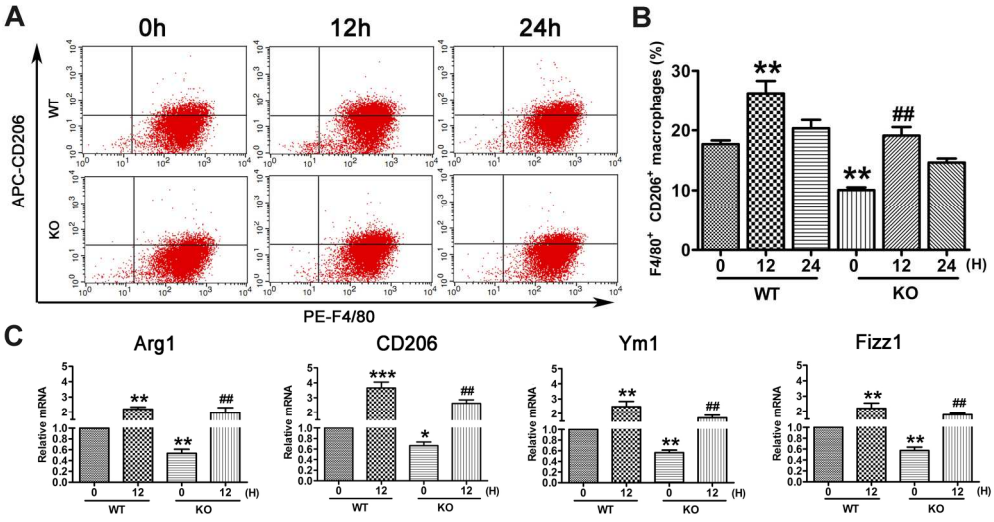

90x46mm (600 x 600 DPI)

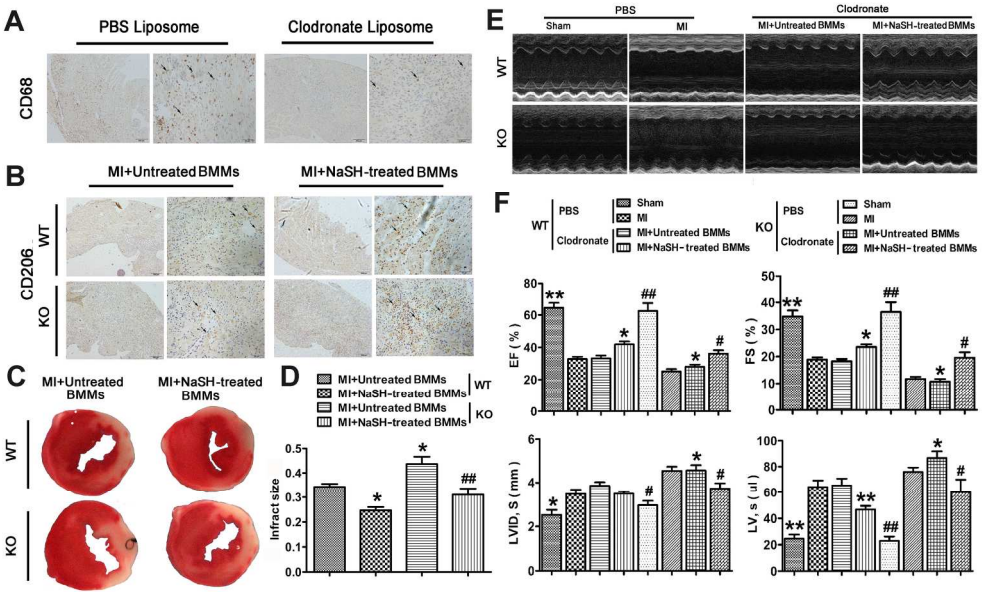

104x62mm (600 x 600 DPI)

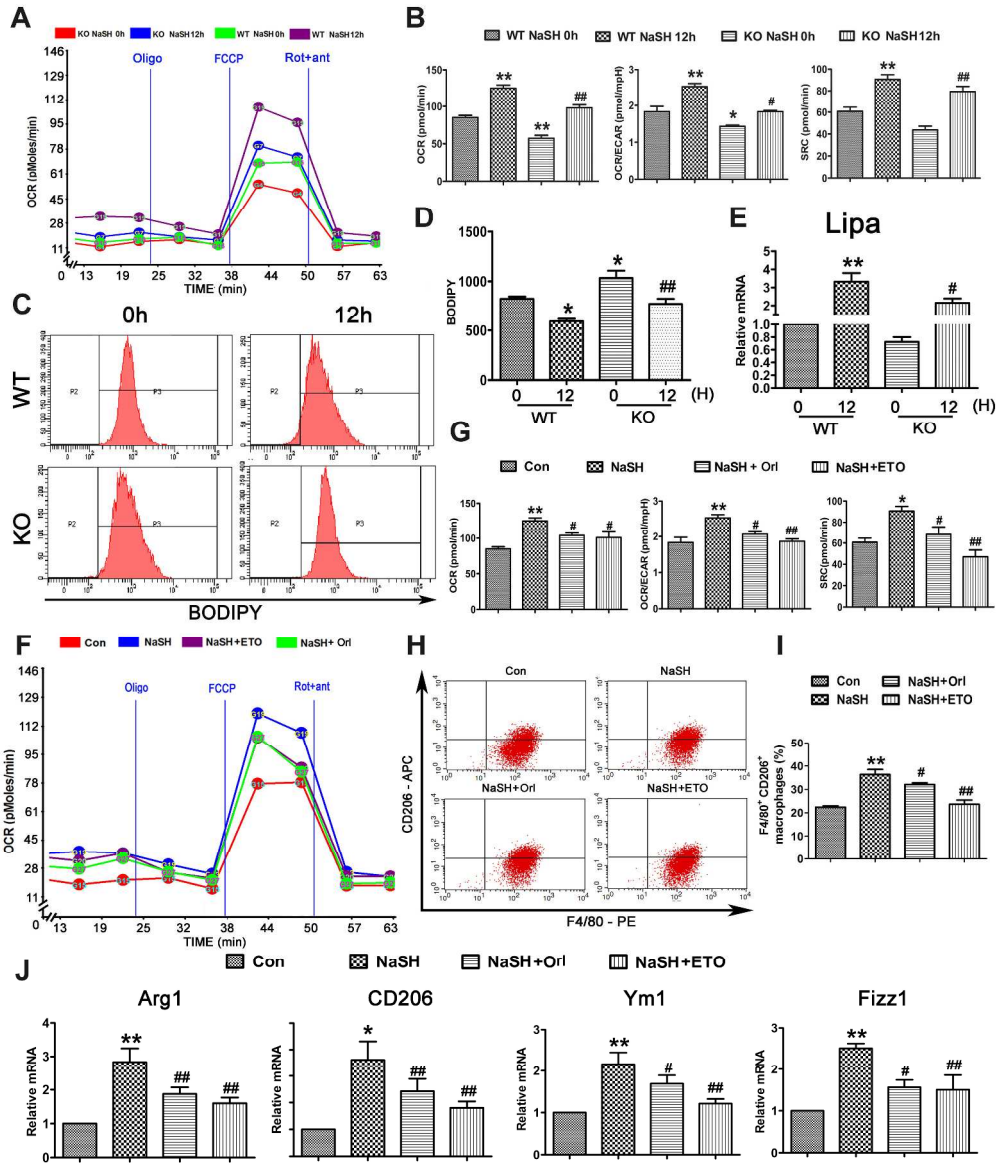

205x242mm (600 x 600 DPI)

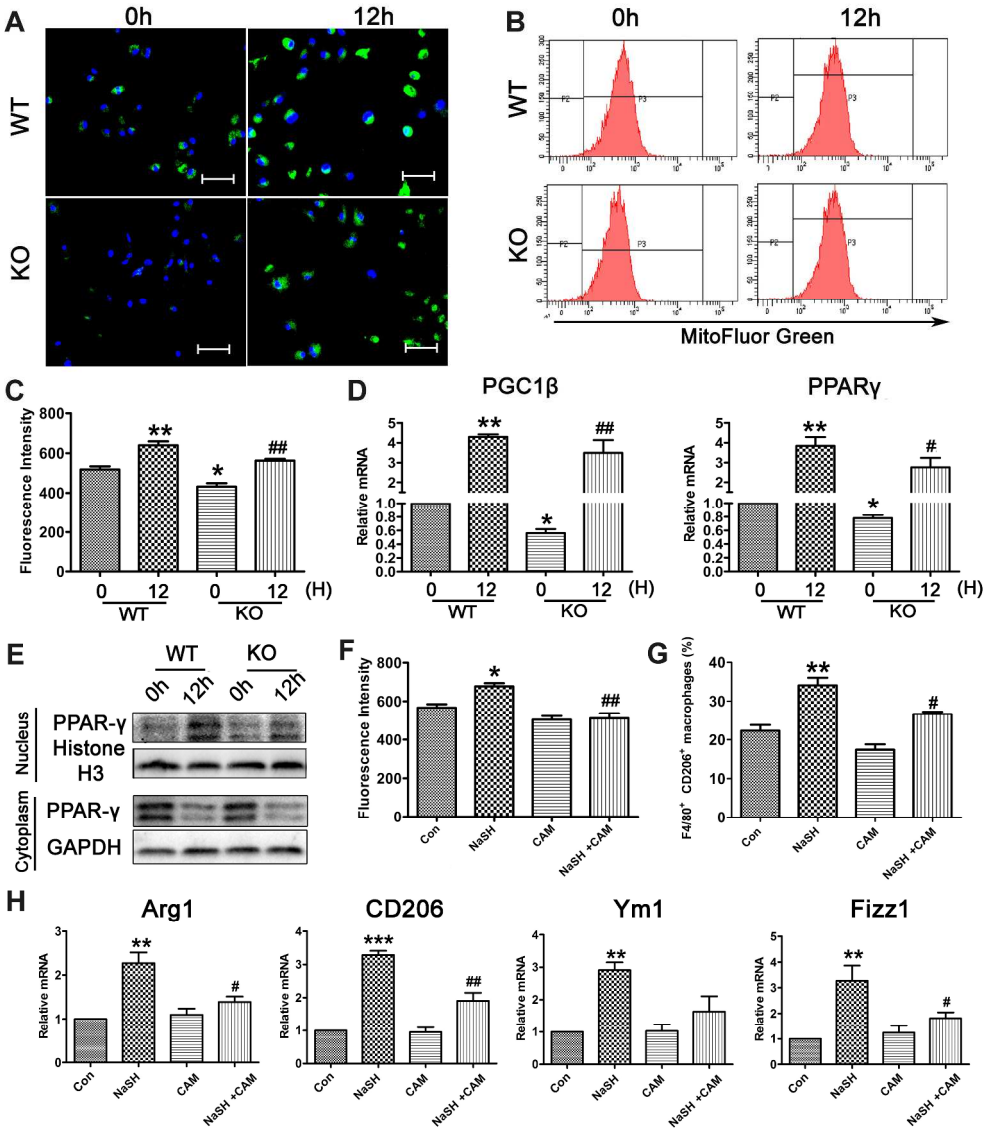

199x226mm (600 x 600 DPI)